Mechanism of the Hydration of Carbon Dioxide: Direct Participation of H2O versus Microsolvation

ARTICLE *in* THE JOURNAL OF PHYSICAL CHEMISTRY A · OCTOBER 2008

Impact Factor: 2.69 · DOI: 10.1021/jp804715j · Source: PubMed

6 AUTHORS, INCLUDING:

Minh Tho Nguyen
University of Leuven
748 PUBLICATIONS **10,856** CITATIONS
SEE PROFILE

Vu Thi Ngan
Quy Nhon University
32 PUBLICATIONS **559** CITATIONS
SEE PROFILE

James Rustad
U.S. Department of Energy
139 PUBLICATIONS **3,086** CITATIONS
SEE PROFILE

David A Dixon
University of Alabama
766 PUBLICATIONS **22,202** CITATIONS
SEE PROFILE

Mechanism of the Hydration of Carbon Dioxide: Direct Participation of H_2O versus Microsolvation

Minh Tho Nguyen,[†,‡] Myrna H. Matus,[†] Virgil E. Jackson,[†] Vu Thi Ngan,[‡] James R. Rustad,[§] and David A. Dixon*[,†]

Department of Chemistry, The University of Alabama, Shelby Hall, Tuscaloosa, Alabama 35487-0336, Department of Chemistry, University of Leuven, B-3001 Leuven, Belgium, and Department of Geology, The University of California-Davis, One Shields Avenue, Davis, California 95616

Received: May 28, 2008; Revised Manuscript Received: July 25, 2008

Thermochemical parameters of carbonic acid and the stationary points on the neutral hydration pathways of carbon dioxide, $CO_2 + nH_2O \rightarrow H_2CO_3 + (n-1)H_2O$, with $n = 1$, 2, 3, and 4, were calculated using geometries optimized at the MP2/aug-cc-pVTZ level. Coupled-cluster theory (CCSD(T)) energies were extrapolated to the complete basis set limit in most cases and then used to evaluate heats of formation. A high energy barrier of ~50 kcal/mol was predicted for the addition of one water molecule to CO_2 ($n = 1$). This barrier is lowered in cyclic H-bonded systems of CO_2 with water dimer and water trimer in which preassociation complexes are formed with binding energies of ~7 and 15 kcal/mol, respectively. For $n = 2$, a trimeric six-member cyclic transition state has an energy barrier of ~33 (gas phase) and a free energy barrier of ~31 (in a continuum solvent model of water at 298 K) kcal/mol, relative to the precomplex. For $n = 3$, two reactive pathways are possible with the first having all three water molecules involved in hydrogen transfer via an eight-member cycle, and in the second, the third water molecule is not directly involved in the hydrogen transfer but solvates the $n = 2$ transition state. In the gas phase, the two transition states have comparable energies of ~15 kcal/mol relative to separated reactants. The first path is favored over in aqueous solution by ~5 kcal/mol in free energy due to the formation of a structure resembling a ($HCO_3^-/H_3OH_2O^+$) ion pair. Bulk solvation reduces the free energy barrier of the first path by ~10 kcal/mol for a free energy barrier of ~22 kcal/mol for the $(CO_2 + 3H_2O)_{aq}$ reaction. For $n = 4$, the transition state, in which a three-water chain takes part in the hydrogen transfer while the fourth water microsolvates the cluster, is energetically more favored than transition states incorporating two or four active water molecules. An energy barrier of ~20 (gas phase) and a free energy barrier of ~19 (in water) kcal/mol were derived for the $CO_2 + 4H_2O$ reaction, and again formation of an ion pair is important. The calculated results confirm the crucial role of direct participation of three water molecules ($n = 3$) in the eight-member cyclic TS for the CO_2 hydration reaction. Carbonic acid and its water complexes are consistently higher in energy (by ~6−7 kcal/mol) than the corresponding CO_2 complexes and can undergo more facile water-assisted dehydration processes.

Introduction

Carbon dioxide has a substantial impact on the environment due to the combustion of fossil fuels.[1] A consensus has emerged that increasing levels of CO_2 in the atmosphere from anthropogenic sources correlate with higher global temperatures.[2] A key constraint on atmospheric CO_2 is the solubility of CO_2 in the oceans. Because of its role in the pH regulation of blood in the human body, the reversible hydration reaction of CO_2 is of biological importance.[3] The photorespiration of plants, consisting of CO_2 uptake and O_2 release from photosynthesis, is a fundamental process in plant physiology.[4]

There are many proposals for sequestering atmospheric CO_2 upon generation. One strategy is injection in deep geological formations or in the ocean.[5,6] CO_2 sequestration can occur by the formation of hydrogen-bonded water cages leading to the formation of gas hydrate clusters (clathrates).[7] Because of the high solubility of carbon dioxide in water, when $CO_2(H_2O)_n$ hydrates dissociate, the dissolution of carbon dioxide in water can form carbonic acid H_2CO_3, its conjugate bases, or both. The hydration reaction of CO_2 forming H_2CO_3 in neutral aqueous media has been the subject of a large number of experimental[8−14] and theoretical[15−23] studies. The properties and dehydration of H_2CO_3 have also been investigated.[24−29] Carbonic acid is a stable discrete molecular species, not only in the gas phase[24] but also in a solid ice matrix at temperatures below that of liquid nitrogen,[26] and likely on acid-treated carbonate mineral surfaces.[13] In the solid conditions, the dimer or oligomers of H_2CO_3 appear to be the more dominant forms.[27] The vibrational spectrum of H_2CO_3 has been analyzed in detail in these earlier studies (see ref 30 for relevant references).

Although a consensus has emerged on the active involvement of a water oligomer $n(H_2O)$, rather than just a water monomer ($n = 1$), in the hydration reaction of CO_2 to form H_2CO_3, the actual number of participating water molecules and the details of their catalytic action remain a matter of debate. From reaction pathways in both the gas phase and the aqueous solution constructed on the basis of molecular orbital calculations at the QCISD(T)/6−31G(d,p)//MP2/6−31G(d,p) level for gas phase systems, in conjunction with both self-consistent-reaction field (SCRF) and polarized continuum (PCM) models and MP2

* Corresponding author. E-mail: dadixon@bama.ua.edu.
† The University of Alabama.
‡ University of Leuven.
§ The University of California-Davis.

10.1021/jp804715j CCC: $40.75
Published on Web 09/25/2008

energies for processes in aqueous solution, Nguyen and co-workers[22] found that the cooperativity and bifunctional catalysis exerted by a second water molecule induces the most important effect on the energy barrier. When the number of water molecules directly involved in the catalytic process is increased, the energy barrier continues to decrease but by smaller amounts. They proposed[22] that the neutral CO_2 hydration proceeds via a water chain mechanism involving $n = 4$ in the gaseous phase and $n = 3$ in neutral aqueous solution. The activation enthalpy was predicted to be ~26 kcal/mol for $n = 3$ in aqueous medium.[22] Subsequently, Liedl and co-workers[27] performed coupled-cluster theory CCSD(T) calculations with the aug-cc-pVDZ and aug-cc-pVTZ basis sets for gas phase systems and MP2/aug-cc-PVDZ/PCM calculations to model the water continuum. These results were used for detailed kinetic analyses of the decomposition rate of H_2CO_3 in aqueous solution. These authors[27] supported the previous findings[22] that four water molecules ($n = 4$), forming a chain, take part in a proton relay facilitating formation of H_2CO_3, and for the reverse process, three water molecules are involved in the decomposition of H_2CO_3. With $n = 4$, the catalytic effect of water for proton transfer reaches a limit on the energy barrier of about ~17−20 kcal/mol in aqueous medium for H_2CO_3 decomposition and ~27−30 kcal/mol for CO_2 hydration. Although there was a subtle difference in the actual number of participating water molecules, both studies[22,27] appeared to agree on the importance of $n = 4$.

In studies reported in 2003, Lewis and Glaser[23] carried out calculations at the MP4/6−311G(d,p) and QCISD(T)/6−31G(d,p) levels, both based on MP2/6−31G(d,p) geometries, and explored other regions of the potential energy surfaces. This level of computation is very close to that used by Nguyen et al.[22] so that the results could be directly compared. Lewis and Glaser[23] proposed an alternative mechanism, which involves a smaller value of $n = 3$ and a different type of transition state. In their transition state, two water molecules effectively assist the proton transfer within a cyclic $(CO_2-H_2O-H_2O)^{\ddagger}$ transition state, whereas the third water molecule interacts from outside with the transition state for $n = 2$ through hydrogen bonds. They[23] found that a proton-shuttle catalysis by two water molecules and microsolvation by the third water is synergistic and the combined effect leads to a zero point corrected barrier of 24.1 kcal/mol, lower than the barrier of 31.8 kcal/mol for the direct three-water catalysis, both starting from a complex of CO_2 with three H_2O molecules. However, their[23] starting point is for a higher energy complex of CO_2 with three H_2O molecules as discussed below. Starting from the asymptote of $CO_2 + 3H_2O$, Nguyen et al. obtain a barrier of 9.8 kcal/mol as compared with a barrier of 8.7 kcal/mol obtained by Lewis and Glaser. Thus, hydrogen bonding in the first solvent shell about the transition state (TS) can affect the energetics slightly more than if the additional water molecule is actually involved in the proton transfer step. A similar difference has been predicted for the molecular mechanism of the hydration process of carbodiimide (HN=C=NH) and carbonyl sulfide (O=C=S), which are either isoelectronic or isovalent with carbon dioxide.[31−34]

Infrared spectroscopy data showed that proton irradiation of icy mixtures of CO_2-H_2O produced solid H_2CO_3.[35] When CO_2-H_2O ice mixtures were irradiated with energetic electrons in an ultrahigh vacuum chamber,[36] H_2CO_3 was found to be the dominant reaction product in the temperature range of 10−60 K. It is likely that the incoming electron induces an O−H bond cleavage in a CO_2-H_2O complex, and the resulting H/OH radicals add successively to a C=O bond of the CO_2 molecule to form H_2CO_3. Such a mechanism differs from the concerted water addition to CO_2 described above.

In view of the importance of the CO_2 hydration reaction to form H_2CO_3, we have performed detailed quantum chemical calculations on the reaction

$$CO_2 + nH_2O \rightarrow H_2CO_3 + (n-1)H_2O \quad (1)$$

for $n = 1-4$. We predicted critical thermochemical parameters and explored relevant portions of the potential energy surfaces in both the gas and the aqueous phases in order to distinguish potentially different mechanisms.

Computational Methods

Electronic structure calculations were carried out by using the Gaussian 03[37] and MOLPRO[38] suites of programs. Enthalpies of formation of the stationary points on the $CO_2 + nH_2O$ reaction pathways were calculated from the corresponding total atomization energy (TAE).[39] We first calculated the electronic energies using coupled-cluster (CCSD(T)) theory[40] extrapolated to the complete basis set limit (CBS) using the correlation-consistent basis sets.[41] Geometry parameters were fully optimized at the second-order perturbation theory (MP2)[42] level with the correlation consistent aug-cc-pVTZ basis set. The fully unrestricted formalism (UMP2) was used for open-shell system calculations done with Gaussian 03. The single-point electronic energies were calculated by using the restricted coupled-cluster R/UCCSD(T) formalism[43−45] in conjunction with the correlation-consistent aug-cc-pVnZ (n = D, T, and Q) basis sets at the (U)MP2/aug-cc-pVTZ optimized geometries. For simplicity, the basis sets are denoted hereafter as aVnZ. The CCSD(T) energies were extrapolated to the CBS limit energies using eq 2:[46]

$$E(x) = A_{CBS} + B\exp[-(x-1)] + C\exp[-(x-1)^2] \quad (2)$$

After the valence electronic energy, the largest contribution to the TAE is the zero-point energy (ZPE). Harmonic vibrational frequencies of each species were calculated at the equilibrium geometry using the MP2/aVTZ method for $n = 1$ and 2 systems and the MP2/aVDZ for $n = 3$ and 4 systems. For CO_2 and H_2O, all fundamental vibrational frequencies are known from experiment.[47,48] Because of the importance of anharmonic corrections in A−H stretches, we used a scaling factor for the O−H stretches of 0.98 obtained for H_2O by averaging the calculated MP2/aVTZ value with the experimental value and dividing by the MP2 value; a similar factor of 0.98 was obtained for the MP2/aVDZ values. These scale factors were subsequently applied to the ZPE(MP2/aVTZ) or ZPE(MP2/aVDZ) values of the molecules, complexes, radicals, ions, and transition state structures.[49]

Additional smaller corrections were included in the TAE calculations. Core-valence corrections (ΔE_{CV}) were obtained at the CCSD(T)/cc-pwCVTZ level of theory.[50] Scalar relativistic corrections (ΔE_{SR}), which account for changes in the relativistic contributions to the total energies of the molecule and the constituent atoms, were included at the CI-SD (configuration interaction singles and doubles) level of theory using the cc-pVTZ basis set. ΔE_{SR} is taken as the sum of the mass−velocity and 1-electron Darwin (MVD) terms in the Breit-Pauli Hamiltonian.[51] Most calculations using available electronic structure computer codes do not correctly describe the lowest energy spin multiplet of an atomic state, as spin−orbit coupling in the atom is usually not included. Instead, the energy is a weighted average of the available multiplets. The spin−orbit corrections are 0.085

kcal/mol for C and 0.223 kcal/mol for O, both from the excitation energies of Moore.[52]

The total atomization energy (ΣD_0 or TAE) of a compound is thus given by the expression

$$\sum D_0 = \Delta E_{elec}(CBS) - \Delta E_{ZPE} + \Delta E_{CV} + \Delta E_{SR} + \Delta E_{SO} \quad (3)$$

By combining our computed ΣD_0 values with the known heats of formation[53] at 0 K for the elements ($\Delta H_f^0(H) = 51.63 \pm 0.001$ kcal/mol, $\Delta H_f^0(C) = 169.98 \pm 0.1$ kcal/mol, and $\Delta H_f^0(O) = 58.99 \pm 0.1$ kcal/mol), we can derive ΔH_f^0 values at 0 K for the molecules in the gas phase. We obtain heats of formation at 298 K by following the procedures outlined by Curtiss et al.[54]

For the $n = 4$ systems due to their size, we calculated the CCSD(T)/aVTZ and MP2/CBS energies and estimated the CCSD(T)/CBS and CCSD(T)/aVQZ energies using the MP2 correction to the CCSD(T)/aVTZ value as[49]

$$\Delta E[CCSD(T)/aVQZ] = \Delta E[CCSD(T)/aVTZ] + (\Delta E[MP2/aVQZ] - \Delta E[MP2/aVTZ]) \quad (4)$$

$$\Delta E[CCSD(T)/CBS] = \Delta E[CCSD(T)/aVTZ] + (\Delta E[MP2/CBS] - \Delta E[MP2/aVTZ]) \quad (5)$$

The effect of solvent normally arises from a combination of an explicit hydrogen-bonded interaction of the solvent molecules with the substrates plus the influence of the bulk surrounding medium. To estimate the latter terms, we employed a polarizable continuum model (PCM).[55] A dielectric constant of $\epsilon = 78.93$ was used for the water bulk; the cavity was created, and the solvation energies were computed using the conductor reaction field (COSMO) formulation.[56] The effects of continuum water on the energetic parameters were calculated using the COSMO method at the MP2/aVTZ level.

Results and Discussion

Total energies are given in Table S1 of Supporting Information; harmonic vibrational frequencies are in Table S2; the ZPE and the thermal corrections are in Table S3, and MP2/aVTZ optimized geometry parameters are given in Table S8. The components used to predict the total atomization energies (ΣD_0) and the ΣD_0 are given in Table S4. The predicted enthalpies of formation at 0 and 298 K are summarized in Table 1, together with the calculated entropies and the available experimental values. Table 2 gives the relative energies for H_2O oligomerization at the MP2 and CCSD(T) CBS limits and also gives the thermodynamic properties of the reactions for forming the water clusters. Table S5 gives the information in Table 2 as a function of the basis set. Table 3 compares the relative energies for the hydration processes $CO_2 + nH_2O$, with $n = 1-3$, and for $CO_2 + (H_2O)_n$, with $n = 2$ and 3 at the MP2 and CCSD(T) CBS levels. Table S6 gives the data in Table 3 as a function of the basis set. Tables 4 lists the calculated thermochemical parameters, and Table 5 gives the activation energies for the CO_2 hydration reactions for $n = 1$ to 3. Table 6 summarizes the calculated results for the $CO_2 + 4H_2O$ and $CO_2 + (H_2O)_4$ reactions and Table S7 gives the data in Table 6 as a function of the basis set.

Thermochemical Parameters of Carbonic Acid and Derivatives. Because of the difficulties in preparing H_2CO_3 under normal conditions, relatively little is known experimentally on its energetics. In a previous theoretical study,[29] we determined thermochemical parameters of H_2CO_3 using the same CCSD(T)/CBS approach, including the standard heat of formation (ΔH_f), gas phase acidity (ΔG_{acid}), and pK_a in aqueous solution. The values for HOCO have been calculated in a similar fashion.[57] We provide additional values in Table 1 for the radical cations, protonated forms, and radical fragments derived by simple bond cleavages (HOCO, HCO_3).

It is well-established that the monomeric H_2CO_3 can exist in three distinct conformations relative to the syn (s) and anti (a) positions of the H(O) atoms with respect to the carbonyl C=O bond. In agreement with numerous previous studies,[16,25,29] the a−a (C_{2v}) conformer is the most stable conformer, 1.5 kcal/

TABLE 1: CCSD(T)/CBS Heats of Formation at 0 and 298 K (kcal/mol) and MP2/aVTZ Entropies (cal/mol-K)

molecule	ΔH_f (0 K)	ΔH_f (298 K)	S
CO_2	−93.6	−93.7	51.10
expt.[a]	−93.97 ± 0.01	−94.05 ± 0.01	51.10 ± 0.03
H_2O	−57.4	−58.1	45.09
expt[a]	−57.10 ± 0.01	−57.80 ± 0.01	45.13 ± 0.01
$(H_2O)_2$	−117.5	−119.4	69.87
$(H_2O)_3$	−182.3	−186.1	79.96
$(H_2O)_4$	−248.6	−254.1	93.12
TS1	−101.3	−103.7	64.74
R1	−152.9	−153.5	81.97
R2	−215.0	−217.0	94.14
TS2	−182.0	−186.6	72.90
P2	−206.4	−210.0	80.78
HOCO	−42.8	−43.6	60.08
expt[b]	−52.5 ± 0.6		
expt[c]	≥ −45.8 ± 0.7	≥ −46.5 ± 0.7	
	≥ −42.7 ± 0.9	≥ −43.4 ± 0.9	
HCO_3	−80.5	−81.9	65.84
HCO_3-	−171.7	−173.3	63.66
H_2CO_3 (C_{2v})	−143.8	−146.3	62.86
H_2CO_3 (C_s), **P1**	−142.3	−144.7	64.42
$H_2CO_3^+$ (C_{2v})	116.9	114.5	64.74
$H_2CO_3^+$ (C_s)	116.8	114.4	66.06
$H_3CO_3^+$ (C_{3v})	45.2	41.9	65.33
$H_3CO_3^+$ (C_s)	39.1	35.7	64.76
R3−3	−279.1	−282.7	105.10
R3−2	−276.0	−278.9	113.04
TS3−3−1	−250.1	−256.3	86.28
TS3−3−2	−249.4	−255.6	86.20
TS3−3−3	−241.2	−247.4	86.19
TS3−2−1	−250.4	−256.4	85.75
TS3−2−2	−247.4	−252.9	89.98
TS3−2−3	−247.5	−253.0	89.62
P3−3	−270.3	−275.3	95.15
P3−2	−273.3	−278.3	93.82

[a] Reference 53. [b] References 53 and 60c. [c] References 60a and 60d.

TABLE 2: Energies, Enthalpies, Energies, and Free Energies for Water Oligomer Formation for $(H_2O)_n$ $n = 2-4$; Energies in kcal/mol and Entropies in cal/mol-K[a]

energy	$2H_2O \rightarrow (H_2O)_2$	$3H_2O \rightarrow (H_2O)_3$	$4H_2O \rightarrow (H_2O)_4$
MP2/CBS	−5.0/−2.8	−16.0/−10.3	−27.9/−19.6
CCSD(T)/CBS	−5.0/−2.8	−15.9/−10.3	−27.5/−19.2
CCSD(T)/CBS [est][b]	[−5.0]/[−2.8]	[−15.9]/[−10.3]	[−27.7]/[−19.4]
ΔH_{rx} (0 K)[c]	−2.7	−10.1	−19.0
ΔH_{rx} (298 K)[d]	−3.2	−11.8	−21.7
ΔS_{rx} [e]	−20.31	−55.32	−87.25
ΔG_{rx} (298 K)	2.9	4.6	4.2

[a] Based on MP2/aVTZ optimized geometries. ZPE's were obtained either from MP2/aVDZ or from MP2/aVTZ harmonic vibrational frequencies (depending on the size of the system), and those corresponding to an O−H stretching were scaled by a factor of 0.98. First value is the electronic energy difference and the second value after the slash includes zero point effects. [b] Estimated by using eq 4. [c] Based on the calculated heats of formation at 0 K. [d] Based on the calculated heats of formation at 298 K. [e] From MP2 values.

TABLE 3: Relative Energies of CO_2 Hydration with $n = 1-3$ H_2O Molecules and with $(H_2O)_n$ ($n = 2$ and 3)[a]

separated system[b]	structure[c]	MP2/CBS	CCSD(T)/CBS[d]
$CO_2 + H_2O$	**R1**	−1.9	−2.0
	TS1	49.1	49.4
$CO_2 + (H_2O)_2$	**R2**	−3.8	−3.9
$CO_2 + 2H_2O$	CO_2-$2H_2O$, **R2**	−6.6	−6.7
	TS2	26.0	26.0
$CO_2 + (H_2O)_3$	**R3−3**	−3.2	−3.3 [−3.3]
	R3−2	0.2	−0.2 [−0.3]
$CO_2 + 3H_2O$	**R3−3**	−13.5	−13.6 [−13.7]
	R3−2	−10.2	−10.5 [−10.6]
	TS3−3−1	15.2	15.2 [15.1]
	TS3−3−2	15.9	15.9 [15.8]
	TS3−3−3	24.0	24.1 [23.9]
	TS3−2−1	15.3	15.0 [14.8]
	TS3−2−2	18.4	18.0 [17.9]
	TS3−2−3	18.4	17.9 [17.8]

[a] Based on MP2/aVTZ optimized geometries. ZPE's were obtained either from MP2/aVDZ or from MP2/aVTZ harmonic vibrational frequencies (depending on the size of the system), and those corresponding to an O−H stretching were scaled by a factor of 0.98. [b] Relative energies are given with respect to the corresponding separated system, including zero-point corrections. [c] Labeling of structures given in Figures 1, 3, 5, and 6. [d] Estimated values in brackets by using eq 4.

TABLE 4: Enthalpies (kcal/mol) at 0 and 298 K, Entropies (cal/mol-K), and Free Energies (kcal/mol) for the $CO_2 + H_2O$ Complexation and Hydration Reactions with $n = 1-3$

complexation reaction	ΔH_{rx} (0 K)[a]	ΔH_{rx} (298 K)[b]	ΔS_{rx}[c]	ΔG_{rx} (298 K)
$CO_2 + H_2O \rightarrow$ **R1**	−1.9	−1.7	−14.21	2.5
$CO_2 + (H_2O)_2 \rightarrow$ **R2**	−3.9	−3.9	−26.83	4.1
$CO_2 + 2H_2O \rightarrow$ **R2**	−6.6	−7.1	−47.13	7.0
$CO_2 + (H_2O)_3 \rightarrow$ **R3−3**	−3.2	−2.9	−25.95	4.8
$CO_2 + (H_2O)_3 \rightarrow$ **R3−2**	−0.1	0.9	−18.01	6.3
$CO_2 + 3H_2O \rightarrow$ **R3−3**	−13.3	−14.7	−81.26	9.5
$CO_2 + 3H_2O \rightarrow$ **R3−2**	−10.2	−10.9	−73.33	11.0
hydration reaction	ΔH_{rx} (0 K)[a]	ΔH_{rx} (298 K)[b]	ΔS_{rx}[c]	ΔG_{rx} (298 K)
$CO_2 + H_2O \rightarrow$ **P1**	8.7	7.1	−31.76	16.6
$CO_2 + 2H_2O \rightarrow$ **P2**	2.0	−0.1	−60.49	17.9
$CO_2 + 3H_2O \rightarrow$ **P3−3**	−4.5	−7.3	−91.21	19.9
$CO_2 + 3H_2O \rightarrow$ **P3−2**	−7.5	−10.3	−92.55	17.3

[a] Based on the calculated heats of formation at 0 K. [b] Based on the calculated heats of formation at 0 K. [c] From MP2 values.

mol more stable than the s−a (C_s) conformer. The s−s (C_{2v}) conformer is much higher in energy because of repulsion of hydrogen atoms and will not be considered further. In the s−a (C_s) conformer, the H atoms have the appropriate orientation to be the primary product of the addition of water into a C=O bond of carbon dioxide, and this conformer will be denoted as **P1** in a following section.

The highest occupied molecular orbital (HOMO) of each H_2CO_3 conformer is an in-plane combination of the oxygen lone pairs, with the largest contribution from the carbonyl oxygen. Removal of an electron from such an orbital gives rise to radical cations having the $^2B_2$ electronic state for the a−a (C_{2v}) conformer and the $^2A'$ electronic state for the s−a (C_s) conformer. Following ionization, both conformers have the same energy within 0.1 kcal/mol, slightly favoring the ionized s−a form ($^2A'$). As a consequence, the C_{2v} form of H_2CO_3 has a marginally larger adiabatic ionization energy (IE_a) than the C_s.

TABLE 5: Barrier Heights (Including Zero Point Energies, kcal/mol), Activation Enthalpies (kcal/mol), Activation Entropies (cal/mol-K), and Activation Free Energies (kcal/mol) for CO_2 Hydration with $n = 1-3$

Reaction	$\Delta E^{\ddagger}$ (0 K)[a]	$\Delta H^{\ddagger}$ (298 K)[b]	$\Delta S^{\ddagger}$[c]	$\Delta G^{\ddagger}$ (298 K)
$CO_2 + H_2O \rightarrow$ **TS1**	49.7	48.0	−31.45	57.4
R1 → TS1	51.6	49.8	−17.23	54.9
$CO_2 + 2H_2O \rightarrow$ **TS2**	26.4	23.3	−68.37	43.7
R2 → TS2	33.0	30.4	−21.24	36.7
$CO_2 + 3H_2O \rightarrow$ **TS3−3−1**	15.7	11.7	−100.09	41.5
R3−3 → TS3−3−1	29.0	26.4	−18.82	32.0
$CO_2 + 3H_2O \rightarrow$ **TS3−3−2**	16.4	12.4	−100.17	42.3
R3−3 → TS3−3−2	29.7	27.1	−18.91	32.7
$CO_2 + 3H_2O \rightarrow$ **TS3−3−3**	24.6	20.6	−100.17	50.5
R3−3 → TS3−3−3	37.9	35.3	−18.91	40.9
$CO_2 + 3H_2O \rightarrow$ **TS3−2−1**	15.4	11.6	−100.62	41.6
R3−2 → TS3−2−1	25.6	22.5	−27.29	30.6
$CO_2 + 3H_2O \rightarrow$ **TS3−2−2**	18.4	15.1	−96.39	43.8
R3−2 → TS3−2−2	28.6	26.0	−23.06	32.9
$CO_2 + 3H_2O \rightarrow$ **TS3−2−3**	18.3	15.0	−96.74	43.8
R3−2 → TS3−2−3	28.5	25.9	−23.41	32.9

[a] Based on the calculated heats of formation at 0 K. [b] Based on the calculated heats of formation at 298 K. [c] From MP2 values.

TABLE 6: Relative Energies Related to CO_2 Hydrogenation with 4 H_2O Molecules and with $(H_2O)_4$[a]

Reaction[b]	MP2/CBS	CCSD(T)/CBS est[c]
$CO_2 + (H_2O)_4 \rightarrow$ **R4−4−1**	−2.7	−2.9
$CO_2 + (H_2O)_4 \rightarrow$ **R4−4−2**	−2.5	−2.7
$CO_2 + (H_2O)_4 \rightarrow$ **R4−2**	1.5	1.0
$CO_2 + (H_2O)_4 \rightarrow$ **R4−3**	1.8	1.3
$CO_2 + 4H_2O \rightarrow$ **R4−4−1**	−22.3	−22.3
$CO_2 + 4H_2O \rightarrow$ **R4−4−2**	−22.1	−22.1
$CO_2 + 4H_2O \rightarrow$ **R4−2**	−18.0	−18.4
$CO_2 + 4H_2O \rightarrow$ **R4−3**	−17.8	−18.1
$CO_2 + 4H_2O \rightarrow$ **TS4−4**	5.6	5.1
R4−4−1 → TS4−4	27.8	27.4
R4−4−2 → TS4−4	27.7	27.2
$CO_2 + 4H_2O \rightarrow$ **TS4−3−3**	2.8	2.4
R4−3 → TS4−3−2	20.6	20.5
$CO_2 + 4H_2O \rightarrow$ **TS4−3−2**	2.6	1.8
R4−3 → TS4−3−3	20.4	19.9
$CO_2 + 4H_2O \rightarrow$ **TS4−3−1**	4.7	4.2
R4−3 → TS4−3−1	22.5	22.3
$CO_2 + 4H_2O \rightarrow$ **TS4−2**	7.6	6.8
R4−2 → TS4−2−1	25.7	25.2

[a] Based on MP2/aVTZ optimized geometries. ZPE's were obtained from MP2/aVTZ harmonic vibrational frequencies, and those corresponding to an O−H stretching were scaled by a factor of 0.98. Relative energies are given with respect to the corresponding separated system, including zero-point corrections. [b] Labeling of structures given in Figure 9. [c] Estimated by using eq 4.

For this quantity, we obtain the following values: $IE_a(H_2CO_3, C_{2v}) = 11.30$ eV and $IE_a(H_2CO_3, C_s) = 11.24$ eV at 0 K. These values can be compared with the experimental IE_a's of some related carbonyl compounds: 10.88 eV for $H_2C(O)$, 10.23 eV for $CH_3CH(O)$, and 11.33 eV for HOCH(O).[58] The methyl group tends to reduce the IE, whereas the hydroxyl substituent increases it by a comparable amount. The IE_a's calculated at the CCSD(T)/CBS level are about 0.03 eV larger than the best

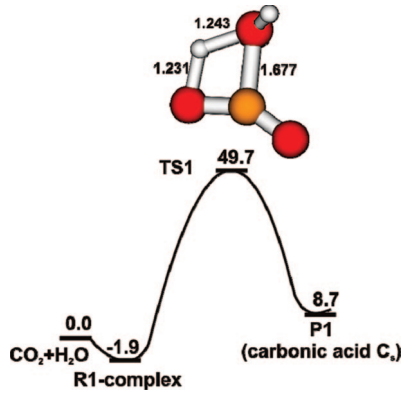

Figure 1. Potential energy profile for $CO_2 + H_2O$ at 0 K. Relative energies in kcal/mol obtained from calculated heats of formation. MP2/aVTZ optimized distances of the transition state **TS1** are given in Å.

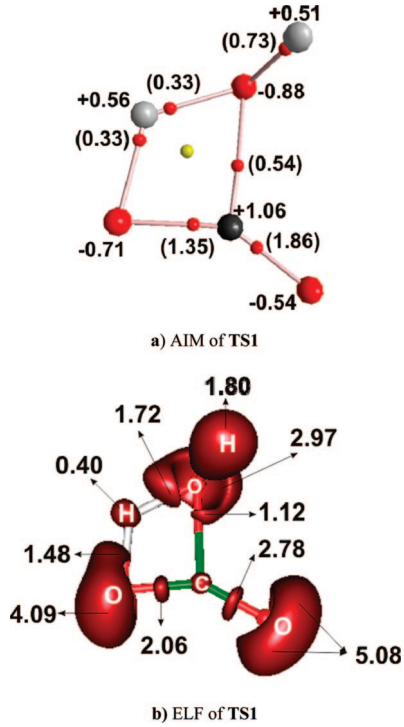

Figure 2. ELF (isosurface = 0.82), natural charges, and Wiberg index orders (in parentheses) were calculated at the B3LYP/aug-cc-pVDZ level. Black sphere is C atom; red sphere is O atom; gray sphere is H; red point is BCP, and yellow point is RCP.

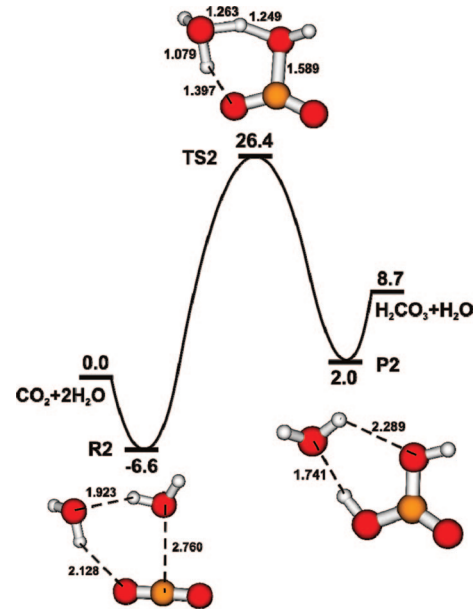

Figure 3. Potential energy profile for $CO_2 + 2H_2O$ at 0 K. Relative energies in kcal/mol obtained from calculated heats of formation. MP2/aVTZ optimized distances of the stationary points are given in Å.

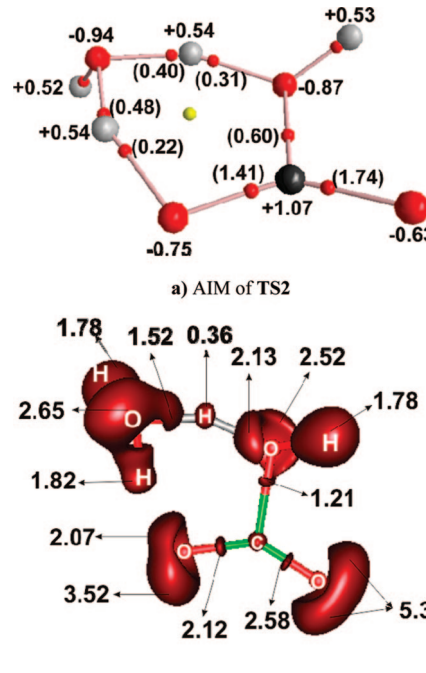

Figure 4. (a) AIM and (b) ELF of the **TS2** of the $CO_2 + 2H_2O$ reaction. See Figure 2 for legend of colors.

experimental values for formaldehyde and acetaldehyde,[59] so our best estimate for the IE_a of H_2CO_3 is about ~0.1 eV smaller than that of formic acid. Thus, substitution of the second OH group for H has very little effect on the IE_a. The stabilization of the HOMO of CH_2O by OH substituents is not additive and is dominated by the first substitution.

Protonation of H_2CO_3 occurs at the carbonyl oxygen yielding two different $(HO)_2C{=}OH^+$ isomers. The lowest-lying protonated forms have a planar C_s structure arising from a−a H_2CO_3 (C_{2v}) and a planar C_3 structure from s−a H_2CO_3 (C_s). We predict that the $(HO)_2C{=}OH^+$ C_s form is 6.2 kcal/mol more stable than the C_3 isomer at 298 K (Table 1). A direct consequence is that a−a H_2CO_3 (C_{2v}) has a higher proton affinity (PA) by 6.3 kcal/mol and PA(H_2CO_3, C_{2v}) = 183.7 kcal/mol. This value can be compared with the PAs of the simple carbonyls, H_2CO, $CH_3CH(O)$, and HOCH(O), which are 170.4, 184.4, and 178.8 kcal/mol, respectively.[58,59] Substitution of the second OH group raises the PA by almost 5 kcal/mol as compared with the increase of ~9 kcal/mol due to substitution of a H by OH in HOCH(O).

The C−O and O−H bond cleavages in H_2CO_3 yield the *trans*-HOCO• ($^2A'$) and HCO_3• ($^2A'$) radicals, respectively. The experimental heat of formation of *trans*-HOCO• is now well-established,[60] and in a previous study, we determined it theoretically using the same CCSD(T)/CBS approach[57] (Table 1). As far as we are aware, no experimental value for the HCO_3• radical is available. Using a heat of formation of 8.84 kcal/mol at 0 K for the OH• radical,[61] we obtain the following adiabatic bond dissociation energies (BDEs) for H_2CO_3 at 0 K: BDE(HCO_2−OH) = 109.8 kcal/mol and BDE(HCO_2O−H) =

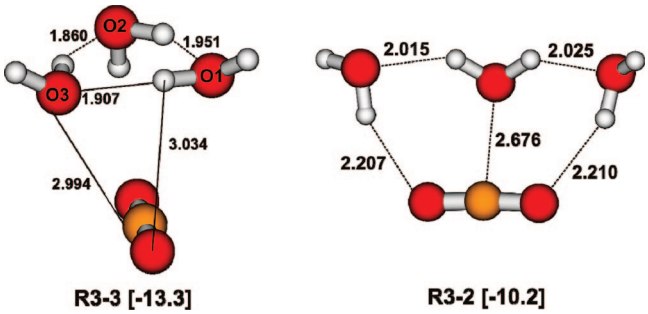

Figure 5. MP2/aVTZ optimized intermolecular distances of two prereaction complexes **R3−3** and **R3−2** of the $CO_2 + 3H_2O$ addition pathways. In brackets are the binding energies, in kcal/mol, obtained from calculated heats of formation with respect to the separated reactant molecules.

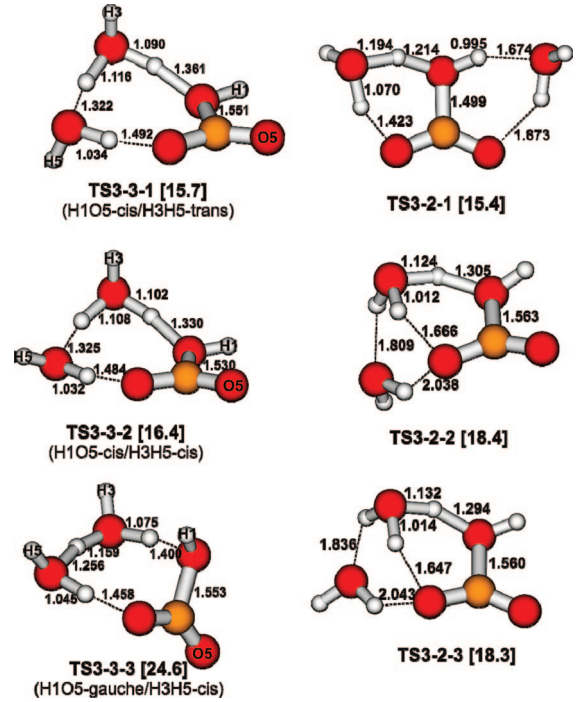

Figure 6. MP2/aVTZ optimized parameters of six TS's related to the $CO_2 + 3H_2O$ pathways. In brackets are the relative energies, in kcal/mol, obtained from calculated heats of formation with respect to the separated reactant molecules.

114.9 kcal/mol. Thus, breaking the C−O bond is slightly favored over breaking the O−H bond. The C−O BDE is larger than the C−O BDE in methanol (90.6 kcal/mol), and the O−H BDE is larger than the O−H BDE in CH_3OH (104.7 kcal/mol).[62]

The results for the carbonate anion HCO_3^- were reported in our previous study,[29] from which a gas phase acidity of $\Delta G_{acid}(H_2CO_3) = 331.3$ kcal/mol and $pK_a = 5.7$ in aqueous solution were predicted. The electron affinity of the carbonate radical is relatively large, $EA(HCO_3\bullet) = 3.95$ eV, consistent with the large resonance stabilization expected for the anion.

Overall, on the basis of the thermochemistry, H_2CO_3 behaves in the gas phase as a normal carboxylic acid with the expected OH substituent effects.

Hydration Reaction Pathways of CO_2. To facilitate the comparison, we adopt the same notation reported previously[22] to describe the stationary points. The letters **Rn**, **TSn,** and **Pn,** with **n** ranging from 1 to 4, refer to the reactant precomplex, transition state, and product complex, respectively. In the labeling for transition structure **TSn-m-p**, **m** (with **m** ≤ **n**) stands for the number of water molecules actually involved in the H transfer, whereas **p** indicates the *p*th structure of this category. The results in Supporting Information show, for either MP2 or CCSD(T), that the effects of enlarging the one-electron basis set are small and, in addition, that most of the correlation energy effects on these energy differences are recovered at the MP2 level as long as the augmented basis sets are used. Tables 4 and 5 list the calculated enthalpies, entropy variations, and free energies of complexation, reaction, and activation. Apart from the expected differences in absolute values, these thermochemical parameters follow the qualitative trends discussed previously.[22,27] In the following discussion, unless otherwise noted, we will employ the relative energies derived from calculated heats of formation at 0 K tabulated in Table 1 for systems with $n = 1$, 2, and 3, and from the estimated CCSD(T)/CBS + ZPE for the $n = 4$ system.

Hydration Reaction for n = 1. The hydration of carbon dioxide by a single water molecule has been the subject of a large body of theoretical studies.[16−20,22,23,26] Figure 1 illustrates the potential energy profile and summarizes the main geometric features of **TS1**. The T-shape of the weak CO_2-H_2O complex R1 in the gas phase has been observed by microwave and molecular beam electric resonance (MBER),[63] and infrared[64] spectroscopies and confirmed by numerous quantum chemical calculations.[65] Previous results for the complexation energy of **R1** range from 2 to 8 kcal/mol with respect to the separated reactants.[65] The most recent binding energy obtained using the MP2/aug-cc-pVTZ method with both basis set superposition error (BSSE) and ZPE corrections amounts to 1.8 kcal/mol, consistent with our present value of 1.9 kcal/mol at 0 K. The binding energy is reduced to 1.7 kcal/mol at 298 K.

The hydration involving the prereaction complex **R1** yielding s−a H_2CO_3 **P1** as product is an endothermic process (8.7 kcal/mol), and there is a substantial energy barrier of 51.6 kcal/mol via **TS1** (49.7 kcal/mol relative to separated reactants). Recent CCSD(T)/VTZ calculations predicted values of 7.4 and 51.3 kcal/mol (relative to separated reactants), respectively, and G2-type calculations predicted comparable values of 8.0 and 52.8 kcal/mol (relative to separated reactants).[27] The earlier QCISD(T)/6−31G** complexation energy is 2.9[22] (2.7)[23] kcal/mol; the barrier from the complex is 51.1[22] (50.8)[23] kcal/mol, and the barrier from separated reactants ($CO_2 + H_2O$) is 48.3[22] (48.1)[23] kcal/mol. Note that there is a cancelation of errors if one uses the activation energy from the complex between all of the methods. This is likely due to BSSE in the smaller basis set calculations. As shown in Supporting Information, there are only small basis set effects on reactions with CO_2 and 1 or 2 H_2O molecules on the order of 1 kcal/mol if diffuse functions are included even at the double-ζ level. There are differences of up to 2 kcal/mol for the reactions of CO_2 with 3 or 4 H_2O molecules as long as diffuse functions are included.

To probe further the electronic mechanism of the concerted addition of water into carbon dioxide, we analyzed the topology of the electron density of **TS1** using the atoms-in-molecules (AIM)[66] and the electron localization function (ELF)[67,68] approaches. The graphical representation of ELF provides a qualitative picture of the molecular basins where electron pairs are concentrated. The integrated electron populations of basins provide a measure to quantify the inherent chemical bonds. Both AIM and ELF calculations were performed at the B3LYP/aug-cc-pVDZ level to generate the electron densities. The Wiberg indices (WI) and NBO atomic charges were also calculated at the same level, and the results are summarized in Figure 2. As expected, **TS1** has a bond critical point (BCP) between both

migrating H and O atoms and a ring critical point for the COHO four-member ring. Within this cycle, both the forming (CO−H) and breaking (HO−H) O−H bonds have similar bond orders (WI = 0.33), whereas formation of the C−OH bond is more advanced (WI = 0.54). Basins covering large domains are located around the O atoms rather than smaller basins for separated lone pairs. When the transition state is reached, part of the electron transfers from the O basin to an H atom to form a H basin with a population of 0.40 electron. The AIM and ELF maps are consistent with each other indicating a large positive charge of the migrating H atom of ∼+0.6. Thus, the hydrogen is best considered as a proton moving between the lone pairs of the two O ends that bear large negative charges. This interaction makes the volume of the lone pair basins smaller than normal.

The influence of bulk aqueous solution on the $CO_2 + H_2O$ reaction pathway has been previously studied.[20,22,26] The methods employed to probe the solvation effects varied from single-point PCM calculations using the gas-phase optimized structures, to full geometry reoptimization of the stationary points using the self-consistent reaction field (SCRF) methods, and Monte-Carlo dynamics simulations. We have used the continuum COSMO approach (Table S9) at the MP2/aVTZ level to predict the effects of solvation on the reaction. We also tested the use of B3LYP/aVTZ with COSMO (Table S9) and found that the absolute electrostatic contribution to the solvation energy differences are within 1 kcal/mol of the COSMO/MP2/aVTZ values except for **R2** which differs by 1.4 kcal/mol. By using gas phase MP2/aVTZ optimized geometries, single-point PCM-COSMO calculations at the MP2/aVTZ level give solvation energies in water of −6.6, −7.4, and −10.0 kcal/mol for the stationary structures **R1**, **TS1**, and **P1**, respectively. These are in good agreement with previous results[22] in that the neutral H_2CO_3 is slightly more stabilized in polar aqueous solution. This is consistent with the size of the dipole moments obtained at the MP2/aVTZ level of 2.39, 2.92, and 3.39 D for **R1**, **TS1**, and **P1**, respectively, as the larger dipole moment should lead to a higher polarization and a larger solvation energy. This makes the addition process less endothermic by 3.4 kcal/mol, and the induced polarization of **TS1** does not lead to a significantly larger stabilization. As a result, the free energy barrier at 298 K for H_2O addition to CO_2 (**R1** → **TS1**) is reduced by only 0.8 kcal/mol by the presence of the solvent. A similar reduction of 0.8 kcal/mol was previously obtained from MP2(SCRF)/6−31G(d,p) calculations using the simpler Onsager model.[22] Even though the barrier reduction is the same in both cases, one should not assume that the simpler model will work as well for other cases without substantial testing.

Unimolecular decomposition of isolated H_2CO_3 **P1** is a high energy process with an energy barrier of 41.0 kcal/mol via **TS1**. The water continuum model tends to stabilize H_2CO_3 more than the TS, which increases the free energy barrier by 2.6 kcal/mol at 298 K.

Hydration Reaction for n = 2. The calculated results are summarized in Figure 3. Preassociation of CO_2 with two water molecules leads to a six-member cyclic complex **R2** with a complexation energy of 6.6 kcal/mol at 0 K (7.1 kcal/mol at 298 K). Earlier QCISD(T)/6−31G(d,p) + ZPE calculations predicted a much larger binding energy of 10.5[22] (9.9) kcal/mol with the difference from the more accurate values being due to BSSE. Note that there is no BSSE in the CBS extrapolations. Our present CCSD(T)/CBS calculations on the water dimer are the same as our previous MP2/CBS calculations[69] showing that the electronic binding energy of $(H_2O)_2$ is about 5.0 kcal/mol. Including a ZPE correction of 2.2 kcal/mol, the resulting adiabatic complexation energy of water dimer is 2.8 kcal/mol at 0 K (see Table 2). The computational/experimental estimate for the binding energy is 3.59 ± 0.5 kcal/mol with an entropy of association of −18.59 ± 1.3 cal/mol-K at 373 K.[70] If we include all of the corrections, we obtain binding energies of 2.7 and 3.2 kcal/mol at 0 and 298 K, respectively, and an entropy of −20.3 cal/mol-K (Table 2).

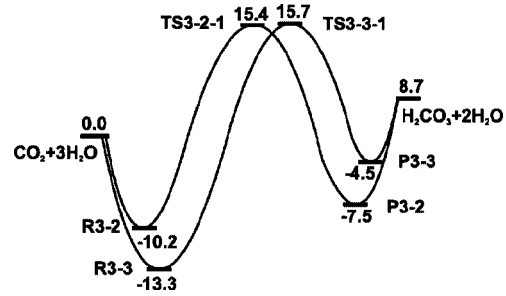

Figure 7. Potential energy profiles for two channels of the $CO_2 + 3H_2O$ addition reaction at 0 K. Relative energies given in kcal/mol obtained from calculated heats of formation.

The second water enhances the interaction with CO_2. The binding energy of **R2** with respect to the separate molecules ($CO_2 + 2H_2O$) is 6.6 kcal/mol at 0 K; this binding energy is less exothermic when it is calculated with respect to the H_2O dimer, 3.9 kcal/mol (Table 4). It is well-established that the second water molecule is a bifunctional acid−base catalyst accelerating H-atom transfer by a six-member cyclic transition structure.[16,18] As shown in Figure 3, this behavior leads to a lower barrier height of 26.4 kcal/mol from separated reactants and 33.0 kcal/mol from prereaction complex **R2**. Previous calculations at the QCISD(T)/6−31(d,p) + ZPE level resulted in barriers of 22.0[22,23] from the separated reactants and 32.5(31.9) kcal/mol from the complex. At the CCSD(T)/VDZ level, the barrier height from $CO_2 + 2H_2O$ is 34.7 kcal/mol, clearly too large as compared with the CCSD(T)/CBS value. Although the barriers from the complex at the QCISD(T)/6−31G** level are comparable to the CCSD(T)/CBS value, the lower level calculation overestimate the binding energy for **R2**, and hence the barrier to separated reactants is too low.

The H_2CO_3 **P1** is stabilized by one water molecule giving complex **P2** with a binding energy of 6.7 kcal/mol so that **P2** is only 2.0 kcal/mol above the $CO_2 + 2H_2O$ limit. Water-assisted decomposition of H_2CO_3 starting from **P2** through **TS2** becomes more favored with a lower energy barrier of 24.4 kcal/mol (Figure 3).

The electron distribution from the AIM and ELF maps displayed in Figure 4 confirms the partial forming and breaking of the bonds when the supersystem reaches **TS2**. The six-member cyclic character of **TS2** is supported by the presence of an RCP, and the existence of bonds is suggested overall by BCP's. The corresponding bond indices vary from 0.2 to 0.6, showing again that the new C−O bond is formed before the new O−H bond. This provides further support for the asynchronous character of bond formation within the concerted addition/H-transfer process. All oxygen centers are negatively charged, whereas all H atoms, migrating or not, bear large positive charges. A global charge transfer of ∼0.3 electron occurs in the direction from $2H_2O$ to CO_2, consistent with the nucleophilic character of the addition reaction. In **TS2**, besides the (O → H) basins already present in **TS1**, the lone pair basin of $O(CO_2)$ interacts with the valence O−H basin of the second water to form a common block, and this interaction reduces

their respective volume. We find that the larger the interaction, the smaller the volume basin. Both AIM and ELF representations of electron density show that, at **TS2**, an important reorganization occurs within the water moiety. The electron density around the second water molecule changes in order to prepare for the subsequent proton relay.

We calculated solvation energies of −8.6, −14.0, and −12.9 kcal/mol for **R2**, **TS2**, and **P2**, respectively. Thus, relative to the gas phase values given in Figure 3, the free energy barrier for the **R2** → **TS2** pathway is reduced by 5.4 kcal/mol, with a predicted free energy barrier of 31.2 kcal/mol in water at 298 K. The barrier to water-assisted concerted decomposition of H_2CO_3 is not substantially improved by the electrostatic interactions of the bulk solvent as the free energy barrier at 298 K for the **P2** → **TS2** channel is decreased by only 1.1 kcal/mol.

Hydration Reaction for n = 3. Figure 5 displays the shape and important intermolecular parameters of both precomplexes **R3**−**3** and **R3**−**2** optimized at the MP2/aVTZ level. **R3**−**3** can be regarded as a complex arising from interaction of a C═O(CO_2) bond with a cyclic water trimer. CO_2 approaches from above the trimer in a nearly perpendicular manner to the plane composed by three water oxygen atoms. Different H and O centers in **R2** remain available for H-bonded interactions with the third water molecule, so several complexes could be formed. We confirm that **R3**−**2** constitutes the most stable form with these types of interactions although it is less stable than **R3**−**3**. **R3**−**2** is built from **R2** with the third H_2O forming an additional H bond with the second C═O(CO_2) bond, which is free in **R2**. **R3**−**2** can be generated from **R1** by adding two water molecules to two different sides. As a result, the three water molecules form a nearly linear chain in which the central H_2O uses both H atoms as H-bond donors. **R3**−**2** can equally be regarded as a complex with two water dimers, but it is not fully symmetrical due to the slight distortion of the central water.

It is well-established that the most stable structure of water trimer is a triangular ring.[71] Extensive MP2/aug-cc-pV6Z calculations[72] led to an electronic binding energy of 15.9 kcal/mol for the cyclic water trimer without ZPE corrections. Our calculations agree with this value and the adiabatic binding enthalpy of water trimer of 10.1 kcal/mol with respect to 3 H_2O (Table 2), based on heats of formation at 0 K. The interaction of the trimer with CO_2 as shown in **R3**−**3** leads to a further stabilization. **R3**−**3** is 13.3 kcal/mol more stable relative to the separated reactants. Thus, complexation of CO_2 to $(H_2O)_3$ gives rise to an additional stabilization of 3.2 kcal/mol (Table 4). With a complexation energy of −10.2 kcal/mol, **R3**−**2** is 3.1 kcal/mol less stable than **R3**−**3** in the gas phase.

We found six transition states at the MP2/aVTZ level for the reaction of three H_2O with CO_2 as shown in Figure 6. These transition states can be categorized as having two H_2O molecules directly involved in the TS with the third water molecule in the first solvation shell leading to **TS3**−**2**−**1**, **TS3**−**2**−**2**, and **TS3**−**2**−**3**. In the second set of TS's, there are three H_2O molecules intimately involved in the proton transfer step, **TS3**−**3**−**1**, **TS3**−**3**−**2**, and **TS3**−**3**−**3**. As confirmed by intrinsic reaction coordinates (IRC)[73] calculations at the HF/aVDZ level, all **TS3**−**3**'s connect with the more stable **R3**−**3**, and the **TS3**−**2**'s connect to the less stable **R3**−**2**. Additional transition states may be present, but we did not find them. To facilitate comparison, relative energies with respect to the separated molecules are also given in Figure 6. The main geometrical features of the TS's have been analyzed in detail previously.[22,23,26] One type of TS's (**TS3**−**3**) differ from each other by the spatial orientation of water hydrogen atoms, whereas the site of H-bonded interactions of the third water molecule makes the difference in the other type of TS's (**TS3**−**2**). For example, **TS-3**−**3**−**1** has a H1O5-*cis* and H3H5-*trans* conformation; **TS3**−**3**−**2** has a H1O5-*cis* and H3H5-*cis* conformation, and **TS3**−**3**−**2** has a H1O5-*gauche* and H3H5-*cis* conformation. Our extensive searches on the potential energy surface confirm the earlier results[22,23,26] that **TS3**−**3**−**1** and **TS3**−**2**−**1** correspond to the lowest-energy structures in their respective categories. For **TS-3**−**3**, there is a relatively short distance of 1.53−1.55 Å for the forming C−O bond and an elongated distance of 1.33−1.40 Å for the broken O−H bond (as compared to the corresponding distances in **TS2**). This geometrical feature is consistent with formation of the $(HOCO_2)^-$ anion and the $H{-}OH_2{-}OH_2^+$ cation. Compared with **TS2**, H-bonded interactions of the third water in **TS3**−**2**−**1** lead to small geometrical changes with the core six-member ring. The main features of the structure regarding the H-transfer mechanism remain in fact unchanged.

The relevant gas phase potential energy profiles are schematically summarized in Figure 7. **TS3**−**3**−**1** and **TS3**−**2**−**1** are found to be almost energetically equivalent, 15.7 and 15.4 kcal/mol above the isolated reactant molecules (CO_2 + $3H_2O$), respectively. The energy barrier for the first channel from the complex **R3**−**3** → **TS3**−**3**−**1** is calculated to be 29.0 kcal/mol. Because the precomplex **R3**−**3** is more stable than **R3**−**2**, the second channel going through **R3**−**2** → **TS3**−**2**−**1** is characterized by a smaller energy barrier of 25.6 kcal/mol. In comparison to the energy barrier of 33.0 kcal/mol for the process with two H_2O via **R2** → **TS2** (Figure 3), both channels show that the effect of an additional water molecule is non-negligible in the gas phase.

The barrier for **R3**−**3** → **TS3**−**3**−**1** has been reported to be 31.8 kcal/mol at the QCISD(T)/6−31G** level, and the barrier for **R3**−**2** → **TS3**−**2**−**1** is 24.1 kcal/mol. Although these values are comparable to the CCSD(T)/CBS values, the shape of the potential energy surface is incorrect at the lower level. The complexation energy for **R3**−**3** is 22.0 kcal/mol, and that for **R3**−**2** is 15.4 kcal/mol at the QCISD(T)/6−31G** level which are too large by 5 to 7 kcal/mol. Hence, the barriers with respect to separated reactants (CO_2 + $3H_2O$) of 9.8 kcal/mol for **TS-3**−**3**−**1** and 8.7 kcal/mol for **TS3**−**2**−**1** at the QCISD(T)/6−31G** level are too low by 5 to 7 kcal/mol. The CCSD(T)/VDZ value[27] of 31.6 kcal/mol for **TS3**−**3** is far too high as compared with the CCSD(T)/CBS value.

Before considering solvent effects, we analyze the electronic reorganization accompanying the two channels. Figure 8 displays the AIM and ELF maps for both **TS3**−**3**−**1** and **TS3**−**2**−**1**. As found in the geometrical parameters, there is a nearly complete addition of an OH group to CO_2, and **TS3**−**3**−**1** is basically split into two moieties having opposite net charges. The ($HOCO_2$) moiety has a negative charge of −0.8 e and the ($H_2O{-}H{-}OH_2$) moiety is positively charged by the same amount. Again, we predict an electron transfer in the direction of $(H_2O)_3$ → CO_2. The basin defining the central H atom of the water moiety contains little electron density (Figure 8b), so that it can be considered as a proton interacting with two water molecules as found for the $(H_5O_2)^+$ cation in the form of a Zundel-ion.[74] **TS3**−**3**−**1** closely resembles an ion pair formed from the bicarbonate anion $(HCO_3)^-$ and the protonated water dimer $(H_2O{-}H{-}H_2O)^+$. The two interfragment bonds are characterized by small bond indices of ∼0.2 (Figure 8a). The electronic landscape in **TS3**−**2**−**1** differs from **TS3**−**3**−**1** but, as expected, is comparable to that of **TS2**. Only negligible charge transfer takes place between the third water and the rest

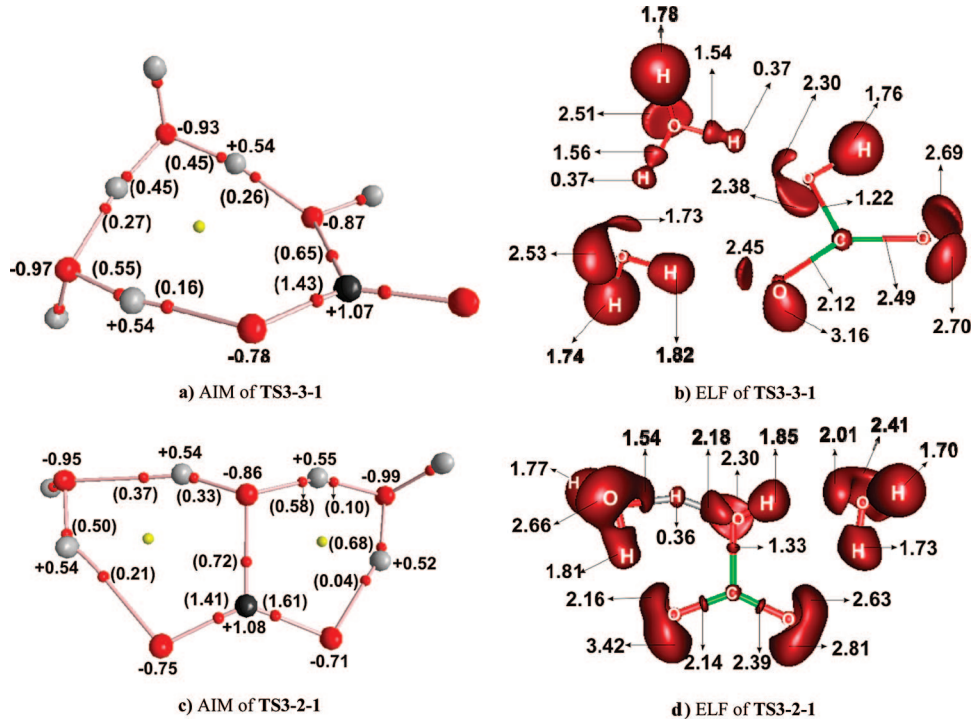

Figure 8. (a) AIM and (b) ELF of **TS3−3−1** and (c) AIM and (d) ELF of **TS3−2−1**. ELF (isosurface = 0.88), natural charges, and Wiberg index orders (in parentheses) were calculated at the B3LYP/aug-cc-pVDZ level. See Figure 2 for legend of colors.

of the supermolecule containing the **TS2** core. This weak interaction leads to only small changes in the electronic distribution.

Our COSMO calculations predict solvation energies of −9.6 and −11.6 kcal/mol for **R3−3** and **R3−2**, respectively. **R3−2** is stabilized more strongly than **R3−3** by electrostatic forces so that both structures could be present in aqueous solutions. This is consistent with the dipole moments of **R3−2** (1.92 D) and **R3−3** (1.26 D). We attempted to find reaction paths that connect **R3−3** and **R3−2**, but we were not successful in identifying a relevant pathway for water migration in the gas phase clusters. Because of the pseudo-ion pair character of the **TS3−3**'s, solvation by a polar solvent is expected to be substantial. Our COSMO calculations result in solvation energies of −19.3, −20.0, and −23.0 kcal/mol for **TS3−3−1**, **TS3−3−2**, and **TS3−3−3,** substantially larger than the solvation energy of −14.9 kcal/mol predicted for all three **TS3−2**'s. This is consistent with the dipole moment for **TS3−3−1** of 6.51 D being larger than the dipole moment of 4.37 D for **TS3−3−2**. As **TS3−3−1** and **TS3−3−2** have approximately the same energy in the gas phase, the energy of **TS3−3−1** in solution is decreased relative to that of **TS3−3−2** by 4.2 kcal/mol relative to the separated reactants. In the gas phase at 298 K, the free energy difference between **R3−2** and **TS3−2−1** is 30.6 kcal/mol, and that between **R3−3** and **TS3−3−1** is 3.0 kcal/mol. In solution, **R3−2** is stabilized by solvent effects more than **R3−3**, whereas **TS3−2−1** is stabilized less than **TS3−3−1** by the solvent. In solution, we predict that the free energy difference between **TS3−3−1** and **R3−3** is 22.3 kcal/mol and that between **TS3−2−1** and **R3−2** 27.3 kcal/mol, so that **TS3−3−1** is the more accessible transition state in solution. The active participation of the third water molecule contributes more efficiently to the catalytic action than as an interacting spectator.

The H-bonded complexes **P3−3** and **P3−2** between H_2CO_3 **P1** and two additional water molecules are calculated to be 4.5 and 7.5 kcal/mol below the separated $CO_2 + 3H_2O$ limit, respectively. The hydration reaction becomes slightly exothermic but remains endothermic when starting from the precomplexes **R3−3** and **R3−2**. The energy barriers for water-assisted decomposition of H_2CO_3 **P3−3** → **TS3−3−1** and **P3−2** → **TS3−2−1** are calculated to be 20.2 and 22.9 kcal/mol, respectively, in the gas phase. In ref 27, an energy barrier of 24.0 kcal/mol was derived from CCSD(T)/aVDZ computations for the **P3−3** → **TS3−3−1** pathway. Our COSMO-PCM calculations with the bulk water continuum predict solvation energies of −15.1 and −12.7 kcal/mol for **P3−3** and **P3−2**, respectively. Inclusion of these solvent effects leads to a free energy barrier at 298 K for **P3−3** → **TS3−3−1** of 17.4 kcal/mol in solution and for **P3−2** → **TS3−2−1** of 22.1 kcal/mol in solution.

Hydration Reaction for n = 4. We first examine the shape and energetics of the water tetramer. The rotation−vibration spectra of this oligomer has been measured and analyzed in detail,[75] and its molecular properties have been the subject of several quantum chemical studies.[76,77] Our calculations concur with the earlier findings that the most stable form of $(H_2O)_4$ is a cycle having S_4 point group symmetry. Each monomer acts as a single H-bond donor and acceptor in which one hydrogen is H-bonded in the ring framework and one is relatively free to distort around the OH−O axis. The free H atoms are alternately up and down with respect to the O−O−O−O square.

The stability of the water tetramer has been predicted using MPn ($n = 2-4$) perturbation theory, with various basis sets.[76,77] Xantheas et al.[78] found MP2/CBS electronic binding energies of 5.0, 15.8, and 27.6 kcal/mol, for the water dimer, trimer, and tetramer, respectively. Our MP2/CBS respective values of 5.0, 16.0, and 27.9 kcal/mol are in excellent agreement with these values. The CCSD(T)/CBS respective values are 5.0, 15.9, and 27.5 kcal/mol (Table 2) showing that the effects of correlation energy beyond second-order are small, <0.5 kcal/mol decreasing the complexation energy, consistent with previous results. Relative to the water trimer discussed in the preceding section, the CBS complexation energy of the water tetramer represents an additional stabilization of ∼9 kcal/mol,

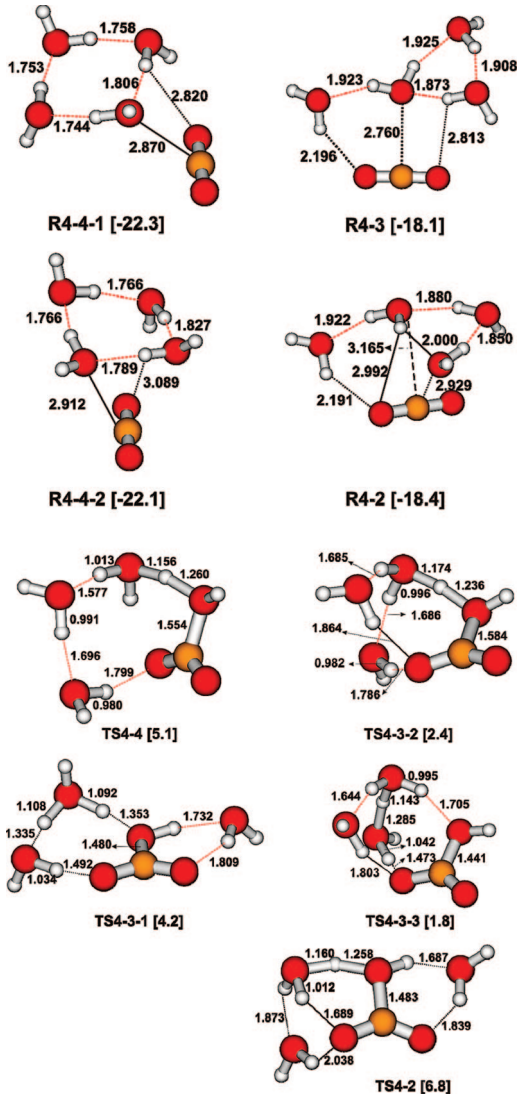

Figure 9. MP2/aVTZ optimized parameters of stationary points for $CO_2 + 4H_2O$. Relative energies in kcal/mol in brackets obtained from CCSD(T)/aug-cc-pVTZ + ZPE calculations with respect to the separated reactant molecules.

yielding a larger increment of −4.8 kcal/mol for H-bond energy per monomer. By considering the cyclic $(H_2O)_4$ as a dimer of $(H_2O)_2$, the dimerization energy of the latter amounts to −13.6 kcal/mol.

To simplify the presentation of data, we focus in this section only on the reactants and corresponding TS's for the water addition to CO_2. As in the case of smaller clusters for $n = 2$ and 3, the products are complexes between H_2CO_3 and water molecules and do not strongly influence the addition mechanism. Figure 9 displays selected MP2/aVTZ optimized geometries of four reactant precomplexes labeled as **R4−4−1**, **R4−4−2**, **R4−3**, and **R4−2**, and five transition states labeled as **TS4−4**, **TS4−3−1**, **TS4−3−2**, **TS4−3−3**, and **TS4−2**. Additional complexes may be present, but we did not find them. Relative energies calculated using different methods are summarized in Table 6 and Table S7 of the Supporting Information. The differences between the energies obtained at all levels, except for MP2/aVDZ, fall within a small range of ±1.0 kcal/mol with respect to the best estimates derived at the CCSD(T)/CBS level.

We located two precomplexes **R4−4** in which the water tetramer conserves its most stable structure and approaches the CO_2 in a nearly parallel plane. The main difference between the two consists in the site of H bond to CO_2, which can be considered as lateral in **R4−4−1** and central in **R4−4−2**. The intermolecular C−O distance of the bond to be formed is long, ∼2.9 Å. Only the structure **R4−4−1** was reported in previous studies.[27,31] In **R4−3**, trimeric water approaches a C═O bond, and the fourth water forms via H bonds with both entities in such a way that a water dimer appears to exist and interacts with the second C═O bond of CO_2. A similar feature is observed for **R4−2** in which a dimer moiety and a trimer moiety joined by a common water molecule, preassociate each with a C═O bond. Each of the complexes denoted **R4−3** and **R4−2** could be the starting point for the addition of either a dimer or a trimer to a C═O bond.

Of the four precomplexes considered, **R4−4−1** is the most stable form, marginally lower in energy than **R4−4−2** by 0.2 kcal/mol and ∼4 kcal/mol more stable than **R4−3** and **R4−2**, which have similar energies. **R4−4−1** has a complexation energy of 22.3 kcal/mol. By considering the value of 19.4 kcal/mol obtained for $(H_2O)_4$ at the same level of calculation, interaction of $(H_2O)_4$ with CO_2 leads to an additional stabilization of 2.9 kcal/mol in **R4−4−1**. The smaller complexation energies of 18.4 and 18.1 kcal/mol in **R4−3** and **R4−2**, respectively, are due to water clusters with higher energies.

Starting from both **R4−4** complexes, we found only one **TS4−4** (Figure 9) which has been observed in previous calculations.[22,27] An interesting feature of **TS4−4** is the emergence of a compact block between CO_2 and two water molecules. The remaining two waters are only loosely bound, even though they are in the TS cycle and effectively take part in the H transfer. Several structures belonging to the class **TS4−3** have been found, and three of these (Figure 9) are the lowest-energy and most representative forms. **TS4−3−1** is composed of **TS3−3−1** (Figure 5) with the fourth water undergoing complex formation at the H1OCO5 site. **TS4−3−2** is related to **TS3−3−2** with the interaction of the additional water in the vicinity of the ring. A similar result is found for **TS4−3−3**, which is derived from **TS3−3−3**. **TS4−3−3** is the lowest energy structure and clearly has a water molecule solvating both the cationic ($H_3OH_2O^+$) and anionic (HCO_3^-) parts of the ion pair formed in the transition state. Again, the difference between **TS4−3−2** and **TS4−3−3** resides in the appearance of a (CO_2−H_2O−H_2O) block in the former and a (HCO_3^-/$H_3OH_2O^+$) ion pair in the latter. **TS4−2** clearly arises from **TS2** (Figure 3) with the two extra water molecules interacting by H bonds in two distinct regions of the complex. In all cases, the free water hydrogen bonds with a **TS3−3** or **TS2** from different regions giving rise to a spectrum of higher energy transition states. Additional transition states may be present in such a complex system with weak interactions, but we did not find them.

All of the transition state energies (Figure 10) lie only 1.8 to 6.8 kcal/mol, as compared with the separated reactant limit ($CO_2 + 4H_2O$). Of the three different types of transition states, the three **TS4−3**'s are consistently lower in energy than **TS4−4** and **TS4−2**. In particular, all of the **TS4−3′s** are energetically quite close to each other. From results listed in Table 6, the energy barriers of the main paths of $CO_2 + 4H_2O$ are

$$\textbf{R4-4-1} \rightarrow \textbf{TS4-4}: E^{\neq} = 27.4 \text{ kcal/mol} \quad (6a)$$

$$\textbf{R4-3} \rightarrow \textbf{TS4-3-1}: E^{\neq} = 22.3 \text{ kcal/mol} \quad (6b)$$

$$\textbf{R4-3} \rightarrow \textbf{TS4-3-2}: E^{\neq} = 20.5 \text{ kcal/mol} \quad (6c)$$

$$\textbf{R4-3} \rightarrow \textbf{TS4-3-3}: E^{\neq} = 19.9 \text{ kcal/mol} \quad (6d)$$

$$\mathbf{R4\text{-}2} \rightarrow \mathbf{TS4\text{-}2}: E^{\neq} = 25.2 \text{ kcal/mol} \quad (6e)$$

The most stable complex **R4−4−1** leads to a reasonably high barrier of 5.1 kcal/mol relative to separated reactants and a quite high barrier relative to **R4−4−1**, just slightly below that for the reaction of three H_2O molecules through the stable complex **R3−3** with a barrier of 29.0 kcal/mol. If complex **R4−3** can be formed, Reaction 6d is the most favored pathway with the lowest energy barrier. This is due to a combination of a higher energy precomplex and a lower energy transition state. If starting from **R4−4−1**, there is a path to **R4−3** and the barrier would be reduced to 24.1 kcal/mol.

A number of conclusions can be drawn from these results. The fact that **TS4−3−1** is 2.5 and 1.8 kcal/mol higher in energy than **TS4−3−3** and **TS4−3−2** is not consistent with the **TS3−2−1** structure where the additional water prefers to interact with the HOCO moiety. This result is consistent with the higher energy of **TS4−2**, which involves both sites of H bonds. The small energy difference of 0.6 kcal/mol between **TS4−3−2** and **TS4−3−3** suggests that both types of H-transfer mechanisms, the compact block and ion pair, are operative and in competition with each other. A comparison of the energies of **TS4−4** and **TS4−3−2**, which have the same type of block, shows that the effect of the fourth water molecule on **TS3−3** is larger if it hydrogen bonds to the complex rather than by direct involvement in the H-transfer process. This result suggests that participation of more water molecules beyond $n = 3$ in the cyclic TS will not lower the barrier and could be counterproductive. Gas phase CO_2 hydration with more than three water molecules involves the direct participation of three water molecules in the cyclic TS with additional molecules preferring to solvate the complex.

Previously, Nguyen et al. found only **TS4−4** and predicted a barrier height of 7.2 kcal/mol from $CO_2 + 4H_2O$ at the MP2/6−311++G** level and a complexation energy of 24.9 kcal/mol. The barrier with respect to the complex of 32.0 kcal/mol is about 5 kcal/mol above the CCSD(T)/CBS value. In their calculations on smaller clusters, their QCISD(T)/6−31G** results had barriers that were ∼7 kcal/mol below the MP2/6−311++G** values so there may be no barrier present with respect to separated reactants. Liedl et al. find barriers of 29.1, 29.8, and 32.7 kcal/mol from $CO_2 + 4H_2O$ for structures similar to **TS4−4**, **TS4−3−1**, and **TS4−3−3**, respectively at the CCSD(T)/VDZ level. These barriers are far too high as compared with the CCSD(T)/CBS values.

Our COSMO calculations show that the solvation energies of all of the prereaction complexes **R4** are comparable, ∼−12 kcal/mol, with a small advantage for **R4−2**. Among the TS's, **TS4−3−1** has the largest solvation energy (−19.4 kcal/mol), and **TS4−2** has the smallest solvation energy (−15.1), with intermediate values for **TS4−3−2** (−15.8), **TS4−4** (-16.1 kcal/mol), and **TS4−3−3** (−18.3). The reaction barriers for reactions 6a−e are all decreased in aqueous medium, and the preference for the reactions 6b and 6d is even larger. The free energy barrier for reaction 6d (**TS4−3−3**) is reduced by 6.5 kcal/mol, yielding a free energy barrier at 298 K of 19.0 kcal/mol for the hydration reaction $CO_2 + 4H_2O$ in bulk water starting from the unstable **R4−3** complex. Adding the energy difference between **R4−4−1** to **R4−3** gives a free energy barrier of 23.2 kcal/mol, very similar to the corresponding value of ∼22.3 kcal/mol for the solvated $CO_2 + 3H_2O$ system from **R3−3** through **TS3−3−1**.

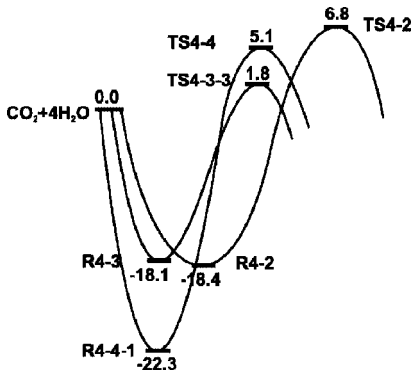

Figure 10. Potential energy profile for the $CO_2 + 4H_2O$ addition reaction at 0 K. Relative energies in kcal/mol obtained from estimated CCSD(T)/CBS and MP2/aVDZ scaled frequencies.

Conclusions

We have investigated the different thermochemical parameters of carbonic acid and the stationary points on the neutral hydration pathways of carbon dioxide, $CO_2 + nH_2O \rightarrow H_2CO_3 + (n-1)H_2O$, with $n = 1-4$, by using high accuracy electronic structure calculations. We find a high energy barrier of ∼50 kcal/mol for the addition of one water molecule to CO_2 ($n = 1$). In agreement with previous studies, this barrier is lowered in cyclic H-bonded systems of CO_2 with water dimer and water trimer in which preassociation complexes are formed with binding energies of ∼7 and ∼13 kcal/mol, respectively. For $n = 2$, a trimeric six-member cyclic transition state has an energy barrier of ∼33 kcal/mol in the gas phase at 0 K and a free energy barrier ∼31 kcal/mol in water as modeled by a continuum solvent, at 298 K relative to the precomplex.

For $n = 3$, two reactive pathways were found. One path proceeds through **TS3−3−1** in which all three water molecules form an eight-member cycle and has a structure consistent with partial ion pair formation. In the second path through **TS3−2−1**, the third water molecule does not directly participate in the H transfer but solvates the reaction region by H bonds with the $n = 2$ stationary points. In the gas phase, the third water molecule equally lowers the energy of the transition state either by direct participation in the supermolecule (**TS3−3−1**) or via microsolvation by H bonds (**TS3−2−1**). In an aqueous medium, the path through **TS3−3−1** becomes energetically more favored and is likely to be predominant. Relative to the precomplex of $CO_2 + 3H_2O$, we predict an energy barrier of ∼29 kcal/mol in the gas phase at 0 K and a free energy barrier of ∼22 kcal/mol in aqueous solution at 298 K. The presence of the ion pair type structure in **TS3−3−1** suggests that the reaction in solution could form HCO_3^-. The pK_a of carbonic acid in aqueous solution is 6.4,[79] which would be consistent with the formation of such an anion in aqueous solution at neutral pH. We are planning to study the direct formation of HCO_3^- in larger water clusters.

For $n = 4$, the transition state incorporating all four water molecules is slightly higher in energy than the transition state in which only a three-water chain takes part in the reaction with the fourth water molecule microsolvating the transition state complex by H bonds. The transition state incorporating only two active water molecules is also energetically less favored. Thus, incorporation of three water molecules in the hydrating chain is necessary, but beyond $n = 3$, additional water molecules no longer reduce the activation energy through direct involvement in the proton transfer process. Relative to the $CO_2 + 4H_2O$ precomplex, an energy barrier of ∼20 and a free energy barrier of ∼19 kcal/mol were predicted in the gas phase at 0 K and in water solution, at 298 K respectively.

Carbonic acid and its water complexes are consistently higher in energy (by ∼6−7 kcal/mol) than the corresponding CO_2

complexes and can undergo a more facile water-assisted dehydration processes. In summary, our high accuracy calculated results clearly confirm the crucial role of a direct participation of three water molecules ($n = 3$) in the eight-member cyclic transition state for CO_2 hydration and show the important effects induced by the solvent via both microsolvation by water molecules and electrostatic stabilization by the continuum.

Acknowledgment. Funding provided in part by the Department of Energy, Chemical Sciences, Geosciences and Biosciences Division, Office of Basic Energy Sciences, U.S. Department of Energy (DOE) under Grant DE-FG02-07ER15840 (geosciences program). D.A.D. is indebted to the Robert Ramsay Endowment of the University of Alabama. M.T.N. thanks the Flemish FWO-Vlaanderen for partly supporting his sabbatical leave at the University of Alabama.

Supporting Information Available: Total MP2 and CCSD(T) electronic energies (E_h) as a function of basis set extrapolated to the complete basis set limit, as well as CCSD(T)/aVQZ and CBS estimates for $n = 4$; MP2/aug-cc-pVDZ entropies and thermal corrections for the structures with $n = 4$ H_2O. Calculated vibrational modes (cm^{-1}). Optimized MP2/aug-cc-pVTZ geometries. COSMO B3LYP and MP2/aug-cc-pVTZ results. MP2/aug-cc-pVTZ intramolecular distances (Å) of **R1, P1, P3−2,** and **P3-3**. This material is available free of charge via the Internet at http://pubs.acs.org.

References and Notes

(1) Koshland, D. E. *Science* **1992**, *258*, 1861.
(2) Mitchell, J. F. B.; Lowe, J.; Wood, R. A.; Vellinga, M *Philos. Trans. R. Soc. A* **2006**, *364*, 2117.
(3) Maren, T. H. *Physiol. Rev.* **1967**, *47*, 595.
(4) Mohr, H.; Schofper, P. Plant Physiology; Springer: Berlin, 1995.
(5) U. S. Department of Energy, Fossil Energy, Carbon Sequestration Program, http://www.fossil.energy.gov/programs/sequestration/.
(6) Broecker, W. S. *Science* **2007**, *315*, 1371.
(7) (a) Circone, S.; Stern, L. A.; Kirby, S. H.; Durham, W. B.; Chakoumakos, B. C.; Rawn, C. J.; Rondinone, A. J. Ishii. *J. Phys. Chem. B* **2003**, *107*, 5529. (b) Yoon, J. H.; Kawamura, T.; Yamamoto, Y.; Komai, T. *J. Phys. Chem. A* **2004**, *108*, 5057.
(8) Zelitch, I *Annu. Rev. Biochem.* **1975**, *44*, 923, and references therein.
(9) Mils, G. A.; Urey, H. C. *J. Am. Chem. Soc.* **1940**, *62*, 1019.
(10) Magid, E.; Turbeck, B. O. *Biochim. Biophys. Acta* **1968**, *165*, 515.
(11) Pocker, Y.; Bjorkquist, D. W. *J. Am. Chem. Soc.* **1977**, *99*, 6537.
(12) Marlier, J. F.; O'Leary, M. H. *J. Am. Chem. Soc.* **1984**, *106*, 5054.
(13) (a) Al-Hosney, H. A.; Grassian, V. H. *J. Am. Chem. Soc.* **2004**, *126*, 8068. (b) Al-Hosney, H. A.; Grassian, V. H. *Phys. Chem. Chem. Phys.* **2005**, *7*, 1266.
(14) Wu, C. Y. R.; Judge, D. L.; Cheng, B. M.; Yih, T. S.; Lee, C. S.; Ip, W. H. *J. Geophys. Res. Planets* **2003**, *108*, 5032.
(15) Jönsson, B.; Karlström, G.; Wenerström, H.; Forsen, S.; Roos, B.; Almlöf, J. *J. Am. Chem. Soc.* **1977**, *99*, 4628.
(16) Nguyen, M. T.; Ha, T. K. *J. Am. Chem. Soc.* **1984**, *106*, 599.
(17) Liang, J. Y.; Lipscomb, W. N. *J. Am. Chem. Soc.* **1986**, *108*, 5051.
(18) Buckingham, A. D.; Handy, N. C.; Rice, J. E.; Somasundram, K.; Dijkgraaf, C. *J. Comput. Chem.* **1986**, *7*, 283.
(19) Nguyen, M. T.; Hegarty, A. F.; Ha, T. K. *J. Mol. Struct. Theochem* **1987**, *150*, 319.
(20) Mertz, K. M. *J. Am. Chem. Soc.* **1990**, *112*, 7973.
(21) Tachibana, A.; Fueno, H.; Tanaka, E.; Murashima, M.; Koizumi, M.; Yamabe, I. *Int. J. Quantum Chem.* **1991**, *39*, 561.
(22) Nguyen, M. T.; Raspoet, G.; Vanquickenborne, L. G.; Van Duijnen, P. Th. *J. Phys. Chem. A* **1997**, *101*, 7379.
(23) Lewis, M.; Glaser, R. *J. Phys. Chem. A* **2003**, *107*, 6814.
(24) Terlouw, J. D.; Lebrilla, C. B.; Schwarz, H. *Angew. Chem., Int. Ed.* **1987**, *26*, 354.
(25) Wright, C. A.; Boldyrev, A. I. *J. Phys. Chem.* **1995**, *99*, 12125.
(26) (a) Hage, W.; Hallbrucker, A.; Mayer, E. *J. Am. Chem. Soc.* **1993**, *115*, 8427. (b) Liedl, K. R.; Sekusak, S.; Mayer, E. *J. Am. Chem. Soc.* **1997**, *119*, 3782. (c) Hage, W.; Liedl, K. R.; Hallbrucker, A.; Mayer, E. *Science* **1998**, *279*, 1332. (d) Loerting, T.; Tautermann, C. S.; Kroemer, R. T.; Kohl, I.; Hallbrucker, A.; Mayer, E.; Liedl, K. R. *Angew. Chem., Int. Ed.* **2000**, *39*, 892.
(27) Tautermann, C. S.; Voegele, A. F.; Loerting, T.; Kohl, I.; Hallbrucker, A.; Mayer, E.; Liedl, K. R. *Chem. Eur. J.* **2002**, *8*, 66.
(28) Kumar, P. P.; Kalinichev, A. G.; Kirpatrick, R. J. *J. Chem. Phys.* **2007**, *126*, 204315.
(29) (a) Alexeev, Y.; Windus, T. L.; Zhan, C.-G.; Dixon, D. A. *Int. J. Quantum Chem.* **2005**, *102*, 775. (b) Erratum.Alexeev, Y.; Windus, T. L.; Zhan, C.-G.; Dixon, D. A. *Int. J. Quantum Chem.* **2005**, *104*, 379.
(30) Tossell, J. A. *Inorg. Chem.* **2006**, *45*, 5961.
(31) Nguyen, M. T.; Raspoet, G.; Vanquickenborne, L. G. *J. Chem. Soc., Perkin Trans. 2* **1999**, 813.
(32) (a) Lewis, M.; Glaser, R. *J. Am. Chem. Soc.* **1998**, *120*, 8541. (b) Lewis, M.; Glaser, R. *Chem. Eur. J.* **2002**, *8*, 1934.
(33) Tordini, F.; Bencini, A.; Bruschi, M.; DeGioia, L.; Zampelle, G.; Fantucci, J. *J. Phys. Chem. A* **2003**, *107*, 1188.
(34) Deng, C.; Li, Q. G.; Ren, Y.; Wong, N. B.; Chu, A. Y.; Zhu, H. J. *J. Comput. Chem.* **2007**, *29*, 466.
(35) More, M. H.; Khanna, R. K. *Spectrochim. Acta* **1991**, *47*, 255.
(36) Zheng, W.; Kaiser, R. I. *Chem. Phys. Lett.* **2007**, *450*, 55.
(37) Frisch, M. J.; Trucks, G. W.; Schlegel, H. B.; Scuseria, G. E.; Robb, M. A.; Cheeseman, J. R. ; Montgomery J.A. Jr.; Vreven, T.; Kudin, K. N.; Burant, J.C.; Millam, J. M.; Iyengar, S. S.; Tomasi, J.; Barone, V.; Mennucci, B.; Cossi, M.; Scalmani, G.; Rega, N.; Petersson, G. A.; Nakatsuji, H.; Hada, M.; Ehara, M.; Toyota, K.; Fukuda, R.; Hasegawa, J.; Ishida, M.; Nakajima, T.; Honda, Y.; Kitao, O.; Nakai, H.; Klene, M.; Li, X.; Knox, J. E.; Hratchian, H. P.; Cross, J. B.; Bakken, V.; Adamo, C.; Jaramillo, J.; Gomperts, R.; Stratmann, R. E.; Yazyev, O.; Austin, A. J.; Cammi, R.; Pomelli, C.; Ochterski, J. W.; Ayala, P. Y.; Morokuma, K.; Voth, G. A.; Salvador, P.; Dannenberg, J. J.; Zakrzewski, V. G.; Dapprich, S.; Daniels, A. D.; Strain, M. C.; Farkas, O.; Malick, D. K.; Rabuck, A. D.; Raghavachari, K.; Foresman, J. B.; Ortiz, J. V.; Cui, Q.; Baboul, A. G.; Clifford, S.; Cioslowski, J.; Stefanov, B. B.; Liu, G.; Liashenko, A.; Piskorz, P.; Komaromi, I.; Martin, R. L.; Fox, D. J.; Keith, T.; Al.Laham, M. A.; Peng, C. Y.; Nanayakkara, A.; Challacombe, M.; Gill, P. M. W.; Johnson, B.; Chen, W.; Wong, M. W.; Gonzalez, C.; Pople, J. A. *Gaussian 03, Revision C.02*; Gaussian, Inc.: Wallingford, CT, 2004.
(38) Werner, H.-J.; Knowles, P. J.; Amos, R. D.; Bernhardsson, A.; Berning, A.; Celani, P.; Cooper, D. L.; Deegan, M. J. O.; Dobbyn, A. J.; Eckert, F.; Hampel, C.; Hetzer, G.; Korona, T.; Lindh, R.; Lloyd, A. W.; McNicholas, S. J.; Manby, F. R.; Meyer, W.; Mura, M. E. ; Nicklass, A.; Palmieri, P.; Pitzer, R. M.; Rauhut, G.; Schütz, M.; Stoll, H.; Stone, A. J.; Tarroni, R.; Thorsteinsson, T. *MOLPRO-2002*, Universität Stüttgart: Stüttgart, Germany; University of Birmingham: Birmingham, United Kingdom, 2002.
(39) (a) Peterson, K. A.; Xantheas, S. S.; Dixon, D. A.; Dunning, T H, Jr. *J. Phys. Chem. A* **1998**, *102*, 2449. (b) Feller, D.; Peterson, K. A. *J. Chem. Phys.* **1998**, *108*, 154. (c) Dixon, D. A.; Feller, D. *J. Phys. Chem. A* **1998**, *102*, 8209. (d) Feller, D.; Peterson, K. A. *J. Chem. Phys.* **1999**, *110*, 8384. (e) Feller, D.; Dixon, D. A. *J. Phys. Chem. A* **1999**, *103*, 6413. (f) Feller, D. *J. Chem. Phys.* **1999**, *111*, 4373. (g) Feller, D.; Dixon, D. A. *J. Phys. Chem. A* **2000**, *104*, 3048. (h) Feller, D.; Sordo, J. A. *J. Chem. Phys.* **2000**, *113*, 485. (i) Feller, D.; Dixon, D. A. *J. Chem. Phys.* **2001**, *115*, 3484. (j) Dixon, D. A.; Feller, D.; Sandrone, G. *J. Phys. Chem. A* **1999**, *103*, 4744. (k) Feller, D.; Dixon, D. A.; Peterson, K. A. *J. Phys. Chem. A* **1998**, *102*, 7053. (l) Dixon, D. A.; Feller, D.; Peterson, K. A. *J. Chem. Phys.* **2001**, *115*, 2576.
(40) Bartlett, R. J.; Musial, M. *Rev. Mod. Phys.* **2007**, *79*, 291, and references therein.
(41) (a) Dunning, T. H. *J. Chem. Phys.* **1989**, *90*, 1007. (b) Kendell, R. A.; Dunning, T. H.; Harrison, R. J. *J. Chem. Phys.* **1992**, *96*, 6796.
(42) Pople, J. A.; Seeger, R.; Krishnan, R. *Int. J. Quant. Chem. Quant. Chem. Symp.* **1977**, *11*, 149.
(43) Rittby, M.; Bartlett, R. J. *J. Phys. Chem.* **1988**, *92*, 3033.
(44) Knowles, P. J.; Hampel, C.; Werner, H.-J. *J. Chem. Phys.* **1994**, *99*, 5219.
(45) Deegan, M. J. O.; Knowles, P. J. *Chem. Phys. Lett.* **1994**, *227*, 321.
(46) Peterson, K. A.; Woon, D. E.; Dunning, T. H., Jr *J. Chem. Phys.* **1994**, *100*, 7410.
(47) Serallach, A.; Meyer, R.; Günthard, Hs. H. *J. Mol. Spectrosc.* **1974**, *52*, 94.
(48) Jacox, M. E. *J. Phys. Chem. Ref. Data* **2003**, *32*, 1.
(49) Nguyen, M. T.; Matus, M. H.; Ngan, V. T.; Haiges, R.; Christe, K. O.; Dixon, D. A. *J. Chem. Phys. A* **2008**, *112*, 1218.
(50) (a) Helgaker, T.; Klopper, W.; Koch, H.; Nagel, J. *J. Chem. Phys.* **1997**, *106*, 9639. (b) Halkier, A.; Helgaker, T; Jørgensen, P.; Klopper, W.; Koch, H.; Olsen, J.; Wilson, A. K. *Chem. Phys. Lett.* **1998**, *286*, 243.
(51) Davidson, E. R.; Ishikawa, Y.; Malli, G. L. *Chem. Phys. Lett.* **1981**, *84*, 226.
(52) Moore, C. E. *Atomic energy levels as derived from the analysis of optical spectra*, Volume*1*, H to V; U.S. National Bureau of Standards Circular 467, U.S. Department of Commerce, National Technical Information Service, COM-72−50282: Washington D.C., 1949.

(53) Chase, M. W., Jr. NIST-JANAF Tablesmed. 4th Ed. *J. Phys. Chem. Ref. Data* **1998**, *9*, 1.
(54) Curtiss, L. A.; Raghavachari, K.; Redfern, P. C.; Pople, J. A. *J. Chem. Phys.* **1997**, *106*, 1063.
(55) (a) Miertus, S.; Scrocco, E.; Tomasi, J. *J. Chem. Phys.* **1981**, *55*, 117. (b) Barone, V.; Cossi, M.; Tomasi, J. *J. Chem. Phys.* **1999**, *107*, 3210.
(56) Eckert, F.; Klamt, A. *AIChE J.* **2002**, *48*, 369.
(57) Feller, D. A.; Dixon, D. A.; Francisco, J. S. *J. Phys. Chem. A* **2003**, *107*, 1604.
(58) NIST, http://webbook.nist.gov/chemistry.
(59) Matus, M. H.; Nguyen, M. T.; Dixon, D. A. *J. Phys. Chem. A* **2006**, *110*, 8864.
(60) (a) Ruscic, B.; Litorja, M. *Chem. Phys. Lett.* **2000**, *316*, 45. (b) Fabian, W. M. F.; Janoschek, R. *J. Mol. Struct. Theochem* **2005**, *713*, 227. (c) Ruscic, B.; Schwarz, M.; Berkowitz, J. *J. Chem. Phys.* **1989**, *91*, 6780. (d) Francisco, J. S. *J. Chem. Phys.* **1985**, *94*, 25.
(61) Ruscic, B.; Wagner, L. B.; Harding, L. B.; Asher, R. L.; Feller, D.; Dixon, D. A.; Peterson, K. A.; Song, Y.; Qian, X.; Ng, C. Y.; Liu, J.; Chen, W.; Schwenke, D. W. *J. Phys. Chem. A* **2002**, *106*, 2727.
(62) Matus, M. H.; Nguyen, M. T.; Dixon, D. A. *J. Phys. Chem. A* **2007**, *111*, 113.
(63) Peterson, K. I.; Klemperer, W. *J. Chem. Phys.* **1983**, *80*, 2439.
(64) (a) Block, P. A.; Marshall, M. D.; Pederson, L. G.; Miller, R. E. *J. Chem. Phys.* **1992**, *96*, 7321. (b) Tso, T. L.; Lee, E. K. C. *J. Phys. Chem.* **1985**, *89*, 1612. (c) Fredin, L.; Nelander, B.; Ribbegard, G. *Chem. Scr.* **1984**, *7*, 72.
(65) (a) Makarewicz, J.; Ha, T. K.; Bauder, A. *J. Chem. Phys.* **1993**, *99*, 3694. (b) Sadlej, J.; Mazurek, P. *J. Mol. Struct. Theochem* **1995**, *337*, 129. (c) Danten, Y.; Tassaing, T.; Besnard, M. *J. Phys. Chem. A* **2005**, *109*, 3250.
(66) (a) Bader, R. F. W. *Atoms in Molecules, A Quantum Theory*; Oxford University Press: New York, 1995. (b) Popelier, P. *Atoms in Molecules. An Introduction*; Prentice Hall: NJ, 2000.
(67) (a) Becke, A. D.; Edgecombe, K. E. *J. Chem. Phys.* **1990**, *92*, 5397. (b) Silvi, B.; Savin, A. *Nature* **1994**, *371*, 63.
(68) Nguyen, M. T.; Nguyen, V. S; Matus, M. H.; Gopakumar, G.; Dixon, D. A. *J. Phys. Chem. A* **2007**, *111*, 679.
(69) Feyereisen, M. W.; Feller, D.; Dixon, D. A. *J. Phys. Chem.* **1996**, *100*, 2993.
(70) Curtiss, L. A.; Frurip, D. J.; Blander, M. *J. Chem. Phys.* **1979**, *71*, 2703.
(71) Keutsch, F. N.; Cruzan, J. D.; Saykally, R. J. *Chem. Rev.* **2003**, *103*, 2533.
(72) Nielsen, I. M. B.; Seidl, E. T.; Janssen, C. L. *J. Chem. Phys.* **1999**, *110*, 9435.
(73) Gonzalez, C.; Schlegel, H. B. *J. Chem. Phys.* **1989**, *90*, 2154.
(74) McCunn, L. R.; Roscioli, J. R.; Johnson, M. A.; McCoy, A. B. *J. Phys. Chem. B* **2008**, *112*, 321, and references therein.
(75) Cruzan, J. D.; Viant, M. R.; Brown, M. G.; Saykally, R. J. *J. Phys. Chem. A* **1997**, *101*, 9022, and references therein.
(76) (a) Kim, K. S.; Dupuis, M.; Lie, G. C.; Clementi, E. *Chem. Phys. Lett.* **1986**, *131*, 451. (b) Schutz, M.; Klopper, W.; Luthi, H. P. *J. Chem. Phys.* **1995**, *103*, 6114. (c) Dunn, M. E.; Evans, T. M.; Kirschner, K. N.; Shields, G. C. *J. Phys. Chem. A* **2006**, *110*, 303, and references therein.
(77) (a) Xantheas, S. S.; Dunning, T. H. *J. Chem. Phys.* **1993**, *99*, 8774. (b) Xantheas, S. S. *J. Chem. Phys.* **1994**, *100*, 7523. (c) Hodges, M. P.; Stone, A. J.; Xantheas, S. S. *J. Phys. Chem. A* **1997**, *101*, 9163.
(78) (a) Xantheas, S. S.; Burnham, C. J.; Harrison, R. J. *J. Phys. Chem.* **2002**, *116*, 1493. (b) Fanourrgakis, G. S.; Xantheas, S. S. *J. Chem. Phys.* **2008**, *128*, 074506.
(79) (a) Schwarzenbach, G. *Helv. Chim. Acta* **1957**, *40*, 907. (b) Hildebrand, J. H. *Principles in Chemistry*; Macmillan: New York, 1940.

JP804715J